

## Filtering Power Divider Based on Lumped Elements

Jin-Xu Xu<sup>1</sup>, Wei-Qiang Pan<sup>2, \*</sup>, Li Gao<sup>3</sup>, and Xiao Lan Zhao<sup>1</sup>

**Abstract**—This paper presents a novel method to design filtering power divider with compact size. Based on lumped elements, a novel topology is proposed and theoretically analyzed. The equivalent power splitting circuits and filtering circuits are characterized by even-odd-mode analysis. Closed-form design equations are obtained, and all the unknown parameters can be derived. Meanwhile, two transmission zeros are produced near the passband edges, resulting in high-selectivity quasi-elliptic responses. For demonstration, a filtering power divider is implemented. The circuit operating at 600 MHz occupies only 15 mm × 14 mm.

### 1. INTRODUCTION

With the rapid development of wireless communication technologies, it is common to integrate multi-standard protocols and combine multiple functions into the same device. Smart phones combining WiFi, cellular phones and Bluetooth are one example of this trend. To realize multiple functions within limited circuit size, miniaturization of RF components becomes extremely important. One method for size reduction is to design multiple function devices, which integrate two or more functions into one device [1–3]. Using this method, the number of components can be reduced and thus the circuit area can be reduced.

In RF front-ends, power dividers and bandpass filters are important building blocks and attract much research interest [4–8]. In many applications, they coexist in the same front-end. Thus, it is necessary to integrate the two functions into one device for miniaturization. In the past, some integrated designs were proposed [9–20]. In [9], the filtering structure is cascaded with the T-junction, resulting in dual functions of power dividing and filtering. In [10], the integration of a single-stage coupled-line bandpass filter and a Wilkinson power divider is reported. However, the skirt selectivity need to be improved. In [11], interdigital coupling sections are utilized to substitute quarter-wavelength transmission lines to achieve filtering power divider response. Besides interdigital coupling sections, bandpass filters are also used to replace the quarter-wavelength transmission lines in Wilkinson power dividers, resulting in single passband responses [12–14]. Unfortunately, they occupy large size. For size reduction, folded quarter-wavelength resonators [15] and capacitor-loaded transmission lines [16] are utilized. Other responses are also studied. For instance, power dividers with dual passband responses [13] and unequal power ratios [17] are reported. In [18–20], UWB power dividers are designed with bandpass responses. Lowpass filters can also be integrated with power dividers to improve the stopband characteristics [21].

The above integrated devices are designed based on transmission lines. In the lower radio frequency range, even the electrical size of the integrated designs is small in terms of the guided-wavelength, and the physical size is still too large in many applications. Compared to transmission line designs, lumped element designs merely require a very small area. On the other hand, the quality factor of the lumped elements is high enough in the lower radio frequency range. Therefore, lumped element designs are

---

*Received 1 August 2014, Accepted 1 September 2014, Scheduled 9 September 2014*

\* Corresponding author: Wei-Qiang Pan (weiqiangpan@126.com).

<sup>1</sup> School of Electronic and Information Engineering, South China University of Technology, Guangzhou 510640, China. <sup>2</sup> Information Network Engineering Research Center, South China University of Technology, Guangzhou 510640, China. <sup>3</sup> City University of Hong Kong Shenzhen Research Institute, Shenzhen 518057, P. R. China.

highly attractive in the lower radio frequency range because of the compact size [5, 22, 23]. For instance, a lumped power divider is designed [5]. However, there is no design about filtering power divider based on lumped elements.

In this paper, a novel method is proposed for designing lumped-element power dividers with quasi-elliptic bandpass responses. The equivalent power splitting circuit and filtering circuit are combined together. The mechanism and theoretical analysis of the proposed circuit is addressed. Closed-form design formulas are derived, which can greatly simplify the design procedures. For demonstration, a power divider is implemented, exhibiting good power dividing performance and high-selectivity bandpass responses.

## 2. DESIGN THEORY

Figure 1 shows the configuration of the proposed power divider with bandpass responses. It consists of seven pairs of lumped-element capacitors and inductors as well as an isolation resistor. The capacitors and inductors can form filtering network and thus dual functions of power division and signal filtering can be realized. The circuit is modified from Wilkinson power dividers and it is symmetrical. Thus, even- and odd-mode analysis can be used to characterize it. According to the network theory of three-port symmetric network, the  $S$ -parameters can be expressed as follow [24]:

$$[S] = \begin{bmatrix} S_{11e} & \frac{1}{\sqrt{2}}S_{21e} & \frac{1}{\sqrt{2}}S_{21e} \\ \frac{1}{\sqrt{2}}S_{21e} & \frac{1}{2}(S_{22e} + S_{22o}) & \frac{1}{2}(S_{22e} - S_{22o}) \\ \frac{1}{\sqrt{2}}S_{21e} & \frac{1}{2}(S_{22e} - S_{22o}) & \frac{1}{2}(S_{22e} + S_{22o}) \end{bmatrix} \quad (1)$$

where  $e$  and  $o$  correspond to even- and odd-mode, respectively. For ideal power dividers, the three ports are perfectly matched and ports 2 and 3 are perfectly isolated, e.g.,  $S_{11} = S_{22} = S_{33} = S_{23} = 0$ . Thus, the following conditions should be satisfied:

$$S_{11e} = S_{22e} = S_{22o} = 0 \quad (2)$$

Meanwhile,  $S_{21e}$  should correspond to the response of a bandpass filter, so that filtering power division responses can be realized. The detailed analysis of the proposed circuit is as follows.

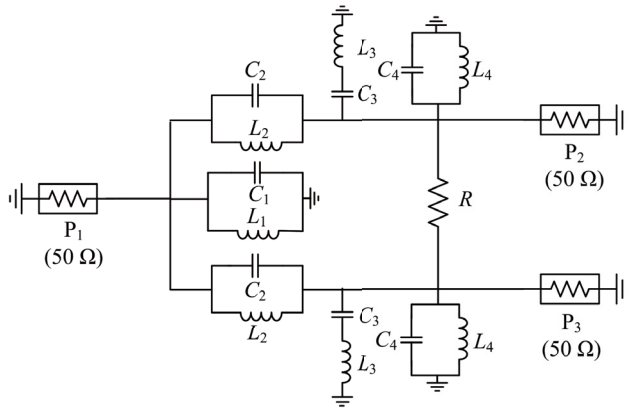


**Figure 1.** The proposed lumped-element power divider with bandpass response.

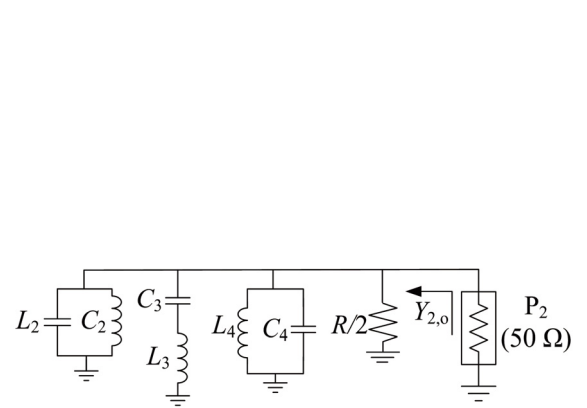


**Figure 2.** The odd-mode equivalent circuit.

### 2.1. Analysis of Odd-Mode Equivalent Circuit

When odd-mode excitation is applied at ports 2 and 3, we can get the equivalent circuit shown in Figure 2. The input admittance for odd-mode circuit  $Y_{2,o}$  can be expressed as

$$Y_{2,o} = \frac{2}{R} + j\omega C_4 + \frac{1}{j\omega L_4} + \frac{j\omega C_3}{1 - \omega^2 L_3 C_3} + j\omega C_2 + \frac{1}{j\omega L_2} \quad (3)$$

For good matching, we can get  $Y_{2,o} = Y_{p2}$ , where  $Y_{p2}$  is the characteristic admittance of port 2 and it equals to 0.02 S. Thus, we can get:

$$\frac{2}{R} = Y_{p2} \quad (4)$$

$$\omega(C_4 + C_2) + \frac{\omega C_3}{1 - \omega^2 L_3 C_3} = \frac{1}{\omega L_4} + \frac{1}{\omega L_2} \quad (5)$$

From Equation (4), the  $R$  is determined as  $100 \Omega$ . From the Equation (5), the operating frequency can be derived. To simplify the calculation, we define  $C_{24} = C_2 + C_4$ ,  $L_{24} = (L_2 L_4)/(L_2 + L_4)$ . Thus, Equation (5) can be simplified.

It is a fourth-order equation, and the operating frequencies can be deduced as

$$\omega = \pm \sqrt{\frac{A \pm \sqrt{A^2 - 4B}}{2}} \quad (6)$$

where  $A = 1/L_3 C_3 + 1/L_{24} C_{24} + 1/L_3 C_{24}$ ,  $B = 1/L_3 C_3 L_{24} C_{24}$ . There may be four roots. Two of them are negative and should be neglected. The other two positive roots correspond to two frequencies. The lower one is utilized as operating frequency  $\omega_0$ . The higher one is denoted as  $\omega_S$ . According to Equation (5) and Vieta's theorem, we can obtain:

$$\omega_0^2 + \omega_S^2 = 1/L_3 C_3 + 1/L_{24} C_{24} + 1/L_3 C_{24} \quad (7)$$

$$\omega_0^2 \omega_S^2 = 1/L_3 C_3 L_{24} C_{24} \quad (8)$$

These two equations can be used to help calculate the design parameters.

### 2.2. Analysis of Even-mode Equivalent Circuit

If even-mode excitation is applied to ports 2 and 3, we can get the equivalent circuit as shown in Figure 3. The impedance of port 1 becomes  $2Z_{p1}$  or  $100 \Omega$ , and the capacitor and inductor close to port 1 are changed to  $C_1/2$  and  $2L_1$ . Thus, the input admittance  $Y_{1,e}$  can be expressed as follows:

$$Y_{1,e} = \frac{j\omega C_1}{2} + \frac{1}{j2\omega L_1} + \frac{\left( j\omega C_2 + \frac{1}{j\omega L_2} \right) \left( \frac{1}{Z_{p2}} + \frac{1}{j\omega L_4} + j\omega C_4 + \frac{j\omega C_3}{1 - \omega^2 L_3 C_3} \right)}{j\omega C_2 + \frac{1}{j\omega L_2} + \frac{1}{Z_{p2}} + \frac{1}{j\omega L_4} + j\omega C_4 + \frac{j\omega C_3}{1 - \omega^2 L_3 C_3}} \quad (9)$$

By substituting (5) to (9), and taking into account that port 1 should be matched, we can obtain:

$$0.5Y_{p1} = Z_{p2} \left( \omega_0 C_2 - \frac{1}{\omega_0 L_2} \right)^2 \quad (10)$$

$$\left( \omega_0 C_1 - \frac{1}{\omega_0 L_1} \right)^2 = 2Y_{p1}^2 \quad (11)$$

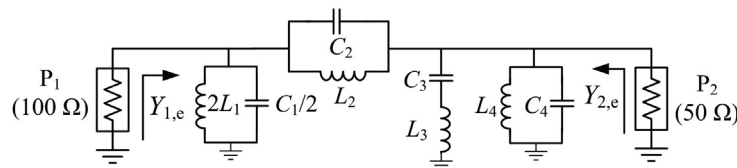


Figure 3. The even-mode equivalent circuit.

With these conditions, the matching of the ports can be satisfied. It does not require the 90-degree phase shift, which is necessary in some other designs [13, 17]. Meanwhile, two transmission zeros are introduced by the configuration. One is due to the parallel resonance of  $C_2$  and  $L_2$ . The other transmission zero is attributed to the serial resonance of  $C_3$  and  $L_3$ . The location of the two transmission zeros can be deduced as follows:

$$\omega_{z1} = 2\pi f_{z1} = \frac{1}{\sqrt{L_2 C_2}} \quad (12)$$

$$\omega_{z2} = 2\pi f_{z2} = \frac{1}{\sqrt{L_3 C_3}} \quad (13)$$

To improve the selectivity, the two transmission zeros are controlled to be located on the two sides of the operating band, namely,  $\omega_{z1} < \omega_0 < \omega_{z2}$ .

Combining (10) and (12), we can calculate  $L_2$  and  $C_2$  as follows:

$$L_2 = \sqrt{2} Z_{p1} \frac{\omega_0^2 - \omega_{z1}^2}{\omega_0 \omega_{z1}^2} \quad (14)$$

$$C_2 = \frac{\omega_0}{\sqrt{2} Z_{p1} (\omega_0^2 - \omega_{z1}^2)} \quad (15)$$

Combining (7), (8) and (13), the  $L_3$ ,  $C_{24}$  and  $L_{24}$  can be determined as follows:

$$L_3 = \frac{1}{C_3 \omega_{z2}^2} \quad (16)$$

$$C_{24} = \frac{C_3 \omega_{z2}^4}{\omega_0^2 \omega_{z2}^2 + \omega_S^2 \omega_{z2}^2 - \omega_{z2}^4 - \omega_0^2 \omega_S^2} \quad (17)$$

$$L_{24} = \frac{\omega_0^2 \omega_{z2}^2 + \omega_S^2 \omega_{z2}^2 - \omega_{z2}^4 - \omega_0^2 \omega_S^2}{C_3 \omega_{z2}^2 \omega_0^2 \omega_S^2} \quad (18)$$

By substituting (14), (15) to (17) and (18),  $C_4$  and  $L_4$  can be calculated as follows:

$$C_4 = C_{24} - C_2 = \frac{C_3 \omega_{z2}^4}{\omega_0^2 \omega_{z2}^2 + \omega_S^2 \omega_{z2}^2 - \omega_{z2}^4 - \omega_0^2 \omega_S^2} - \frac{\omega_0}{\sqrt{2} Z_{p1} (\omega_0^2 - \omega_{z1}^2)} \quad (19)$$

$$L_4 = \frac{\sqrt{2} Z_{p1} (\omega_0^2 - \omega_{z1}^2) (\omega_0^2 \omega_{z2}^2 + \omega_S^2 \omega_{z2}^2 - \omega_{z2}^4 - \omega_0^2 \omega_S^2)}{\sqrt{2} Z_{p1} (\omega_0^2 - \omega_{z1}^2) C_3 \omega_{z2}^2 \omega_0^2 \omega_S^2 - (\omega_0^2 \omega_{z2}^2 + \omega_S^2 \omega_{z2}^2 - \omega_{z2}^4 - \omega_0^2 \omega_S^2) \omega_0 \omega_{z1}^2} \quad (20)$$

In the above section, the issues of operating frequency, isolation and port matching have been analyzed. For a power divider with bandpass responses, the equivalent filtering circuit should be considered. For the even-mode circuit, it is equivalent to a bandpass filter consisting of lumped capacitors and inductors. The bandwidth is defined as  $\Delta f$ , and the 3-dB frequency points are defined as  $f_1 = f_0 - \Delta f/2$ ,  $f_2 = f_0 + \Delta f/2$ . Therefore, the following equations should be satisfied:

$$S_{21e}(L_1, C_3)|_{f=f_1, f_2} = 0.707 \quad (21)$$

Here,  $S_{21e}$  can be calculated by:

$$S_{21e} = \sqrt{1 - \Gamma_{1,e}^2} \quad (22)$$

$$\Gamma_{1,e} = \frac{0.5Y_{p1} - Y_{1,e}}{0.5Y_{p1} + Y_{1,e}} \quad (23)$$

It is noted that the parameters  $C_1$ ,  $L_3$ ,  $C_4$  and  $L_4$  can be represented by  $L_1$  and  $C_3$  as indicated by the Equations (11), (16), (19) and (20). The  $C_2$  and  $L_2$  are determined by (14) and (15). Thus, the  $S_{21e}$  is the function of  $L_1$  and  $C_3$ . Therefore, by solving the Equation (21), the two parameters  $L_1$  and  $C_3$  can be obtained. Then, all the unknowns can be conventionally calculated by using a simple MATLAB program.

### 3. CIRCUIT IMPLEMENTATION

Based on the design theory, we can briefly summarize the design methodology as follows. It is assumed that the circuit specifications  $f_0$ ,  $\Delta f$ ,  $f_{Z1}$  and  $f_{Z2}$  are given.

Step 1: According to the given operating frequency  $f_0$  and lower transmission zero  $f_{Z1}$ , the parameter  $C_2$  and  $L_2$  can be determined by (14) and (15).

Step 2: Referring to the equations of (11), (16), (19) and (20), the parameters  $C_1$ ,  $L_3$ ,  $L_4$  and  $C_4$  can be represented by  $L_1$ ,  $C_3$  and the given upper transmission zero  $f_{Z2}$ .

Step 3: By substituting  $C_1$ ,  $L_3$ ,  $L_4$ ,  $C_4$ ,  $L_1$ ,  $C_3$ ,  $f_1$  and  $f_2$  to (21), we can calculate the values of  $L_1$  and  $C_3$ .

Step 4: Substituting the value of  $L_1$  and  $C_3$  to (11), (16), (19) and (20), the value of  $C_1$ ,  $L_3$ ,  $L_4$  and  $C_4$  can be obtained. Thus, all values of the eight parameters have been obtained.

To verify the above process, a design is taken as an example. The filter specifications are given as follows:  $f_0 = 600$  MHz,  $\Delta f = 100$  MHz,  $f_{Z1} = 300$  MHz,  $f_{Z2} = 900$  MHz. Following the step 1,  $C_2$  and  $L_2$  can be calculated with the values of 5.005 pF and 56.29 nH. Then  $L_1$  and  $C_3$  can be calculated with the values of 3.064 nH and 15.95 pF in the step 3. After that,  $C_1$ ,  $L_3$ ,  $L_4$  and  $C_4$  can be obtained as follows:  $C_1 = 15.95$  pF,  $L_3 = 1.963$  nH,  $C_4 = 2.285$  pF,  $L_4 = 2.027$  nH. Thus, all the initial values are obtained. The simulation results of this ideal case are shown in Figure 4. Good power division and bandpass responses are observed. The operating frequency is located at 601 MHz and 3-dB bandwidth is 102 MHz. Two transmission zeros are located at 300 MHz and 900 MHz. The three ports are well matched. The isolation is over 40 dB at the center frequency. The good agreement between the prediction and simulation validates the analysis and design procedures.

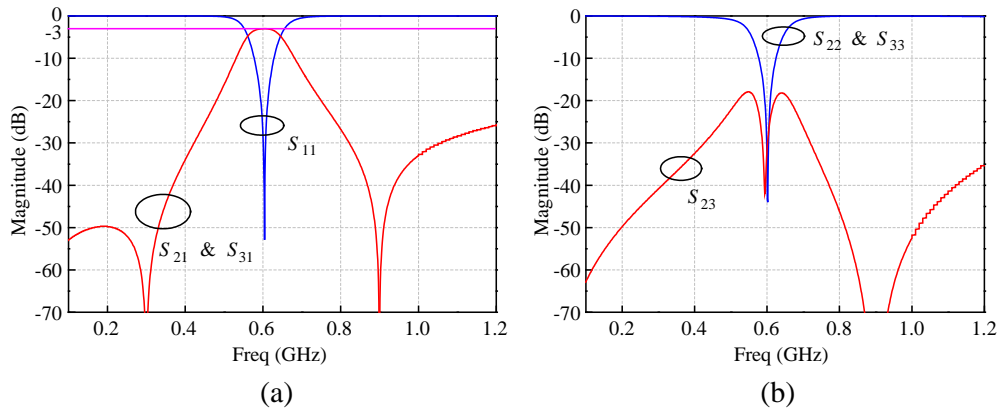


**Figure 4.** Simulated results of ideal case. (a)  $S_{11}$ ,  $S_{21}$  and  $S_{31}$ . (b)  $S_{22}$ ,  $S_{33}$  and  $S_{23}$ .

To demonstrate it, a circuit is implemented on the substrate with a relative dielectric constant of 3.38, loss tangent of 0.0027 and thickness of 0.81 mm. The lumped-element parameters can be calculated using the above design procedure. Due to the parasitic effects of practical elements, the ideal inductors and capacitors are replaced by the practical SMD Murata ones with lower quality factor and thus the insertion loss becomes higher. Then short length microstrip lines are used to connect them. Finally, fine tuning is used to get good performance. The final values are selected as  $L_1 = 3.3$  nH,  $C_1 = 11$  pF,  $L_2 = 27$  nH,  $C_2 = 5$  pF,  $L_3 = 2.2$  nH,  $C_3 = 9$  pF,  $L_4 = 2.2$  nH,  $C_4 = 1$  pF,  $R = 120 \Omega$ . These values are different with the calculated ones due to two reasons. Firstly, the specifics of the calculated model and the final implemented one are different. The frequencies of the transmission zeros in Figure 4 is 300 and 900 MHz. In order to enhance the selectivity, we move the locations close to the passband. These lead to the difference of the element values. Secondly, the difference is due to the parasitic effects and the introduction of the added transmission lines. The initial element values are obtained by ideal model, while in practice, the parasitic effects exist. Therefore, the implemented element values need to be changed, resulting in different values. We obtain these values by the following manners. We can first use Murata inductors to replace the ideal ones and perform fine tuning. After that we use Murata

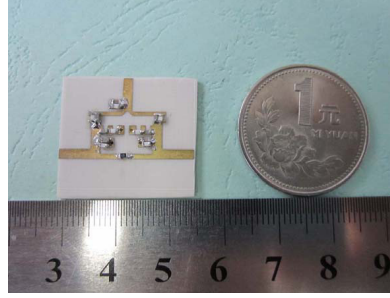


**Figure 5.** Photograph of the fabricated circuit.

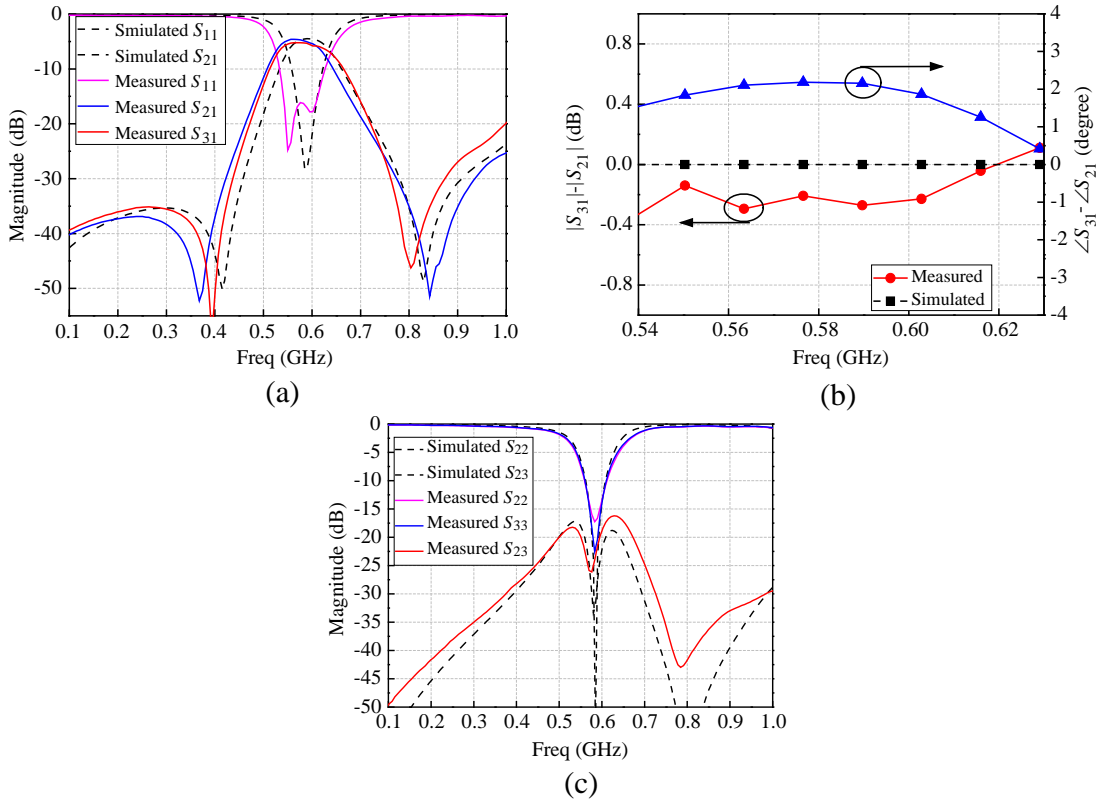


**Figure 6.** Simulated and measured results (a)  $S_{11}$ ,  $S_{21}$  and  $S_{31}$ . (b) Amplitude and phase imbalance. (c)  $S_{22}$ ,  $S_{23}$  and  $S_{33}$ .

capacitors to replace the ideal ones and then conduct fine tuning. In this way, we can get the final values of practical components. The fabricated photograph is shown in Figure 5 and the total size is  $15 \text{ mm} \times 14 \text{ mm}$ .

The simulation and measurement are accomplished by Agilent ADS and 8753ES network analyzer, respectively. Figure 6 shows the simulated and measured results. Good power division and bandpass responses are observed. The center frequency is located at 585 MHz and the bandwidth is 105 MHz or 17.9%. The  $S_{21}$  and  $S_{31}$  are 4.6 and 4.8 dB, respectively. Compared with the cascaded filter and power divider, this design exhibits lower insertion loss. Two transmission zeros are generated close to the passband edges. Within the passband, the amplitude imbalance is less than 0.3 dB and the phase imbalance is less than 2.5 degree. The in-band return loss is greater than 15 dB. The isolation is around 26 dB at the center frequency and better than 16 dB within the whole band.

#### 4. CONCLUSION

This paper has presented a novel method for designing compact power divider with bandpass responses. Both theory and experiments have been provided, showing that the filtering and power splitting circuits are highly integrated and the proposed devices can exhibit the dual functions with good performance. The closed-form design equations have been derived, which greatly simplify the design procedures. Due to the use of lumped elements, the circuit size is very compact. With these features, the proposed method is attractive for highly-integrated circuit designs in the UHF band.

#### ACKNOWLEDGMENT

This work was supported by the NSFC under grant Nos. 61271060 and 61271209.

#### REFERENCES

1. Mansour, G., M. J. Lancaster, P. S. Hall, P. Gardner, and E. Nugoolcharenlap, "Design of filtering microstrip antenna using filter synthesis approach," *Progress In Electromagnetics Research*, Vol. 145, 59–67, 2014.
2. Zuo, S.-L., W.-J. Wu, and Z.-Y. Zhang, "A simple filtering-antenna with compact size for WLAN application," *Progress In Electromagnetics Research Letters*, Vol. 39, 17–26, 2013.
3. Chen, X., F. Zhao, L. Yan, and W. Zhang, "A compact filtering antenna with flat gain response within the passband," *IEEE Antennas Wireless Propag. Lett.*, Vol. 12, 857–860, 2013.
4. Bei, L., S. Zhang, and K. Huang, "A novel dual-band multi-way power divider using coupled lines," *Progress In Electromagnetics Research C*, Vol. 37, 41–51, 2013.
5. Kawai, T., H. Mizuno, I. Ohta, and A. Enokihara, "Lumped-element quadrature Wilkinson power divider," *Asia Pacific. Microw. Conf.*, 1012–1015, 2009.
6. Li, J. C., Y. L. Wu, Y. A. Liu, J. Y. Shen, S. L. Li, and C. P. Yu, "A generalized coupled-line dual-band Wilkinson power divider with extended ports," *Progress In Electromagnetics Research*, Vol. 129, 197–214, 2012.
7. Gao, L. and X. Y. Zhang, "High selectivity dual-band bandpass filter using a quad-mode resonator with source-load coupling," *IEEE Microw. Wireless Compon. Lett.*, Vol. 23, 474–476, 2013.
8. Jun, S. and K. Chang, "Compact microstrip bandpass filter using miniaturized hairpin resonator," *Progress In Electromagnetics Research Letters*, Vol. 37, 65–71, 2013.
9. Singh, P. K., S. Basu, and Y.-H. Wang, "Coupled line power divider with compact size and bandpass response," *Electronics Lett.*, Vol. 45, 892–894, 2009.
10. Tang, X. and K. Mouthaan, "Filter integrated Wilkinson power dividers," *Microw. Opt. Tech. Lett.*, Vol. 52, 2830–2833, 2010.
11. Shao, J.-Y., S.-C. Huang, and Y.-H. Pang, "Wilkinson power divider incorporating quasi-elliptic filters for improved out-of-band rejection," *Electronics Lett.*, Vol. 47, 1288–1289, 2011.
12. Cheong, P., K.-I. Lai, and K.-W. Tam, "Compact Wilkinson power divider with simultaneous bandpass response and harmonic suppression," *IEEE MTT-S Int. Microwave Symp. Dig.*, 1588–1591, 2010.
13. Li, Y. C., Q. Xue, and X. Y. Zhang, "Single- and dual-band power divider integrated with bandpass filters," *IEEE Trans. Microw. Theory Tech.*, Vol. 61, 69–76, 2013.
14. Lu, Y. L. and G. L. Dai, "Novel filtering power divider using multiple internal resistors," *Progress In Electromagnetics Research Letters*, Vol. 45, 75–80, 2014.
15. Chen, C.-F., T.-Y. Huang, T. M. Shen, and R.-B. Wu, "Design of miniaturized filtering power dividers for system-in-a-package," *IEEE Trans. Component Packag. Manufact. Technol.*, Vol. 3, 1663–1672, 2013.
16. You, C.-W. and Y.-S. Lin, "Miniature on-chip bandpass power divider with equal ripple response and wide stopband," *IET Microw. Antenna and Propag.*, Vol. 6, 1461–1467, 2012.

17. Deng, P.-H. and L.-C. Dai, "Unequal Wilkinson power dividers with favorable selectivity and high-isolation using coupled-line filter transformers," *IEEE Trans. Microw. Theory Tech.*, Vol. 60, 1520–1529, 2012.
18. Wong, S. W. and L. Zhu, "Ultra-wideband power divider with good in-band splitting and isolation performances," *IEEE Microw. Wireless Compon. Lett.*, Vol. 18, 518–520, 2008.
19. Xiao, L., H. Peng, and T. Yang, "Bandpass-response power divider with high isolation," *Progress In Electromagnetics Research Letters*, Vol. 46, 43–48, 2014.
20. Gao, S. S., S. Sun, and S. Xiao, "A novel wideband bandpass power divider with harmonic-suppressed ring resonator," *IEEE Microw. Wireless Compon. Lett.*, Vol. 23, 119–121, 2013.
21. Choi, M.-G., H.-M. Lee, Y.-H. Cho, X.-G. Wang, and S.-W. Yun, "Design of Wilkinson power divider with embedded low-pass filter and cross-stub for improved stop-band characteristics," *IEEE MTT-S Int. Microwave Symp. Dig.*, 1–4, 2011.
22. Elsbury, M. M., P. D. Dresselhaus, N. F. Bergren, C. J. Burroughs, S. P. Benz, and Z. Popovic, "Broadband lumped-element integrated  $N$ -way power dividers for voltage standards," *IEEE Trans. Microw. Theory Tech.*, Vol. 57, 2055–2063, 2009.
23. Hou, J.-A. and Y.-H. Wang, "Design of compact 90 and 180 couplers with harmonic suppression using lumped-element bandstop resonators," *IEEE Trans. Microw. Theory Tech.*, Vol. 58, 2932–2939, 2010.
24. Pozar, D. M., *Microwave Engineering*, 3rd Edition, John Wiley & Sons, 2005.